Available online at www.sciencedirect.com
SCIENCE DIRECT
Journal of Inorganic Biochemistry 96 (2003) 321–330
JOURNAL OF Inorganic Biochemistry
www.elsevier.com/locate/jinorgbio

Mechanism of insulin sensitization by BMOV (bis maltolato oxo vanadium); unliganded vanadium (VO_4) as the active component

Kevin G. Peters*, Mike G. Davis, Brian W. Howard, Matthew Pokross, Vinit Rastogi, Conrad Diven, Kenneth D. Greis, Elaine Eby-Wilkens, Matthew Maier, Artem Evdokimov, Shari Soper, Frank Genbauffe

Procter & Gamble Pharmaceuticals, Cardiovascular Research, Health Care Research Center, 8700 Mason-Montgomery Road, Mason, OH 45040, USA

Received 28 January 2003; received in revised form 28 May 2003; accepted 29 May 2003

Abstract

Organovanadium compounds have been shown to be insulin sensitizers in vitro and in vivo. One potential biochemical mechanism for insulin sensitization by these compounds is that they inhibit protein tyrosine phosphatases (PTPs) that negatively regulate insulin receptor activation and signaling. In this study, bismaltolato oxovanadium (BMOV), a potent insulin sensitizer, was shown to be a reversible, competitive phosphatase inhibitor that inhibited phosphatase activity in cultured cells and enhanced insulin receptor activation in vivo. NMR and X-ray crystallographic studies of the interaction of BMOV with two different phosphatases, HCPTPA (human low molecular weight cytoplasmic protein tyrosine phosphatase) and PTP1B (protein tyrosine phosphatase 1B), demonstrated uncomplexed vanadium (VO_4) in the active site. Taken together, these findings support phosphatase inhibition as a mechanism for insulin sensitization by BMOV and other organovanadium compounds and strongly suggest that uncomplexed vanadium is the active component of these compounds.

Keywords: BMOV; Phosphatase; Vanadate; HCPTPA; PTP1B; Insulin; Diabetes

1. Introduction

The insulin receptor belongs to a family of growth factor receptors termed receptor tyrosine kinases (RTKs) [1]. Ligand binding of the insulin receptor results in activation of the kinase domain leading to autophosphorylation on specific tyrosine residues [2–6]. Autophosphorylation in turn further activates the kinase domain and provides binding sites for the recruitment and subsequent phosphorylation of signaling molecules such as IRS-1 (insulin receptor substrate 1) which drive the cellular responses important for insulin action. Thus, the regulation of tyrosine phosphorylation of the insulin receptor likely plays an important role in insulin action.

Recent findings demonstrate that protein tyrosine phosphatases (PTPs) are negative regulators of insulin receptor signaling. For example, PTP1B and LAR (leukocyte antigen related-protein) are upregulated in patients with Type 2 diabetes [7,8]. Overexpression of PTP1B, LAR or HCPTPA in cultured cells attenuates insulin receptor activation and signaling [9–14]. Conversely, reducing PTP1B activity in vivo using either antisense oligos or gene targeting results in enhanced insulin receptor signaling and improved insulin sensitivity and glucose tolerance [15–17]. These findings show that PTPs, PTP1B in particular, may be good therapeutic targets for treatment of insulin resistance states such as type 2 diabetes.

Vanadium compounds have gained attention because of their insulin mimetic activity [18–20]. In cultured cell lines, vanadium compounds enhance insulin receptor activation and downstream signaling [21–26]. In animal models of diabetes, vanadium compounds improve insulin sensitivity resulting in decreased levels of plasma glucose and insulin [27–37]. Importantly, this enhanced insulin sensitivity occurs in the absence of weight gain that complicates therapy with exogenous insulin and the recently developed PPAR-γ (peroxisome proliferator-activated receptor) agonists.

One likely mechanism for the insulin mimetic activity of vanadium compounds relates to their potent inhibition of

*Corresponding author. Tel.: +1-513-622-0834; fax: +1-513-622-1433.
E-mail address: peters.kg@pg.com (K.G. Peters).

0162-0134/03/$ – see front matter
doi:10.1016/S0162-0134(03)00236-8

PTPs [23,38,20]. A variety of vanadium compounds have been shown to directly inhibit a wide range of PTPs including PTP1B [39,40]. Recently, organovanadium compounds have been shown to have superior insulin mimetic activities compared to sodium orthovanadate [41,23,42,43]. Currently the reasons for the superior activity of organovanadium compounds are not clear but may relate to better bioavailability of these compounds or more potent activity at the enzyme active site.

To gain further insight into the insulin mimetic actions of organovanadium compounds, we have explored the mechanism by which a novel organovanadium compound, bismaltolato oxovanadium (BMOV), inhibits phosphatase activity. Like other organovanadium compounds BMOV was a reversible, competitive phosphatase inhibitor. Importantly, BMOV inhibited phosphatase activity in cultured cells and enhanced the autophosphorylation of the insulin receptor in vivo. NMR and X-ray crystallographic approaches demonstrated that the active component of BMOV is most likely to be uncomplexed vanadium (VO_4). These studies support the hypothesis that organovanadium compounds exert their insulin mimetic activities, at least in part, by phosphatase inhibition. In addition, these studies suggest that the reason for improved efficacy of organovanadium compounds vs. inorganic vanadium most likely relates to bioavailability rather than increased potency at the phosphatase enzyme active site.

2. Materials and methods

2.1. Materials

Bismaltolato oxovanadium was synthesized according to published procedures [44]. Briefly, vanadyl sulfate (2.00 g, 12.3 mmol) was dissolved in 100 ml H_2O and 3-hydroxy-2-methyl-4-pyrone (maltol) (2.48 g, 19.7 mmol) was added at once. Using a pH meter, 1 N NaOH was added dropwise with stirring into the solution until pH 8.50. The mixture was refluxed overnight and the product was crystallized upon cooling to room temperature. After filtering, the product was vacuum dried and stored in a desiccator.

2.2. Molecular cloning of HCPTPA and PTP1B and production of recombinant HCPTPA

cDNA clones encoding HCPTPA and PTP1B were generated by PCR from human placenta cDNA purchased from Clontech. Primers used for HCPTPA were: forward with XhoI site 5′-CCGCTCGAGGAAGATGGCGGAACAG-3′, reverse with NotI site 5′-ATAAGAATGCGGCCGCCTGGAACGTGATTACACACCG-3′, and for PTP1B: forward with EcoRI site 5′-GGAATTCATGGAGATGGAAAAGGAG-3′, reverse with NotI site 5′-TGCGGCCGCCTATGTGTTGCTGTTG-3′. Subsequent PCR products were subcloned into pPCR-Script (Stratagene) and sequenced before being further subcloned for bacterial (HCPTPA; see next paragraph) or mammalian (PTP1B; see Section 2.3) expression.

The HCPTPA cDNA was cloned into a pET-28a vector (Novagen) and expressed in E. coli strain BL-21(DE3) (Stratagene) at 37 °C. Induced cells were lysed by sonication in 20 mM tris–HCl (pH 7.5) on ice. Soluble protein was loaded onto a Q Sepharose FF column (Pharmacia), washed with lysis buffer and eluted with a linear 0–1 M NaCl gradient. Peak fractions were pooled, adjusted to 1.5 M $(NH_4)_2SO_4$ and loaded onto a phenyl sepharose 6 FF column (Pharmacia). The column was washed with loading buffer, then eluted with a 1.5–0 M $(NH_4)_2SO_4$ gradient in 20 mM tris–HCl (pH 7.5). Peak fractions were pooled, concentrated and further purified on a Superdex 75 column (Pharmacia) in 25 mM Hepes (pH 8.0) 150 mM NaCl.

2.3. Phosphatase assays

Kinetic assays were done using the recombinant phosphatases and fluorogenic small molecule substrate 6,8-difluoro-4-methylumbelliferyl phosphate (DiFMUP, Molecular Probes) (10 μM) was incubated for 15 min with nM concentrations of phosphatase in buffer containing 10 mM Na Acetate, 150 mM NaCl, 5 mM DTT, pH 6. Recombinant HCPTPA was produced as described above (Section 2.2) and PTP1B was purchased from Biomol (SE-332). The resulting phosphatase product was measured at 355/460 nm (ex/em) using a Victor V plate reader (Wallac). Inhibitors (0.002–40 μM) were pre-incubated with phosphatase for 10 min prior to addition of DiFMUP substrate. IC50 curves were generated using Excel-Fit. Kinetic analysis was performed using 3 concentrations of inhibitor to calculate velocity over a range of DiFMUP concentrations (0–400 μM) and Lineweaver–Burke plots were used to evaluate inhibitor mechanism.

To measure phosphatase activity and inhibition in cultured cells a cDNA clone encoding PTP1B (see Section 2.2 above) was subcloned into the expression vector pcDNA3.1 (Invitrogen). HEK 293 h cells (Gibco) were transfected with the PTP1B plasmid using lipofectamine2000 (Gibco). Expression was detected by western at 48 h using an anti-PTP1B antibody (PTP1B-Ab1; Calbiochem). Phosphatase activity was detected by treating the cells with 50 μM DiFMUP for 30 min and measuring fluorescence at 355/460 nm (ex/em) using a Victor V plate reader. BMOV was pre-incubated with cells for 30 min before substrate addition.

2.4. Mass spectrometric analysis

2.4.1. Perfusion HPLC-coupled mass spectrometry

Screening of intact protein masses after reaction with various vanadium inhibitors was done by perfusion chromatography (POROS II R/H, 300 μm i.d.) coupled to a

Sciex API 165 single quadrupole Mass Spectrometer in positive, electrospray ionization mode. After a 1 min hold at 1% CH_3CN/0.02%TFA the protein was eluted with a linear gradient to 85% CH_3CN over 2 min.

2.4.2. Capillary HPLC-coupled, electrospray ionization tandem mass spectrometry (CAPLC-ESI-MS/MS)

Trypsin digested samples were separated on a Pepmap C18, 3 μm, 300 μm i.d.×50 mm column (LCPackings) using an LCPackings Ultimate capillary LC system with a gradient of 2% B to 50% B in 30 min at 4 μl/min where A = 0.1% formic acid/2%CH_3CN; B = 0.1% formic acid/98%CH_3CN. The effluent from the LC was coupled directly to a custom-built micro-ESI interface on a Finnigan LCQ^{Deca} ion-trap mass spectrometer. Positive ion spectra were collected in data dependent mode such that an MS/MS fragmentation spectrum was obtained for each peak detected above a threshold 1×10^5.

2.5. In vivo insulin receptor activation

To assess the effect of BMOV on insulin receptor activation in-vivo, fasted rats (250–300 g) were infused with either saline or BMOV for 5 min followed immediately by a 10-min infusion with either saline or insulin via a carotid artery catheter. Animals were euthanized and the heart was removed, flash frozen in liquid nitrogen and stored at −80 °C until assayed. For analysis of insulin receptor activation, 250 mg of frozen tissue was homogenized in RIPA buffer: 50 mM Tris (pH 7.5), 150 mM NaCl, 1 mM EDTA, 1% NP-40, 0.25% SDS, 1 mM Na_3VO_4, 1 mM NaF, 10 nM Okadaic acid plus 1 complete protease inhibitor tablet (Roche). Homogenates were centrifuged at ~21,000×*g* speed for 30 min at 4 °C. Supernatants were recovered and protein concentrations were determined by the BCA assay (Pierce). One milligram (1 mg) of extracted protein was pre-cleared with 25 μl of protein A/G-Plus agarose beads (Santa Cruz Biotech.) for 1 h at 4 °C. Insulin receptor beta was immunoprecipitated from the pre-cleared lysate using 10 μg of an anti-insulin receptor beta antibody (C-19, Santa Cruz Biotech) at 4 °C overnight. The complex was precipitated using 25 μl of protein A/G-Plus agarose beads (Santa Cruz Biotech.) for 1 h at 4 °C. Afterwards the beads were sedimented at ~21,000×*g* for 1 min, washed once in cold lysis buffer and bound proteins eluted by boiling for 5 min in 30 μl of 1× sample buffer (50 mM Tris–HCl (pH 6.8), 10% glycerol, 2% SDS, 0.1 mM DTT, 0.1% bromphenol blue). The samples were centrifuged for 1 min at maximum speed and 20 μl of the supernatant was loaded onto an 8% SDS–PAGE gel, transferred to PVDF membranes and phosphotyrosine western blotting was performed using anti-phosphotyrosine antibody (PY99, Santa Cruz Biotech.) diluted 1:1000 in 2.5% bovine serum albumin in TBS–0.1% Tween-20. Signal was detected using ECL (Amersham). After exposure the blots were stripped and re-probed with anti-insulin receptor beta (C-19, Santa Cruz Biotech). Resulting films were scanned and quantitated using Quantity-One software (Bio-Rad).

2.6. NMR studies

Uniformly ^{15}N-labeled HCPTPA was overexpressed in *Escherichia coli* BL21(DE3) strain grown in a minimal media containing ^{15}N-NH_4Cl (1 g/l) (Isotec Inc., Miamisburg, OH) as the sole nitrogen source.

Expression and purification details were the same as previously published [45]. NMR samples contained ~167 μM HCPTPA in 50 mM acetate buffer (pH 5.1). NMR experiments were recorded at 298 K using a Varian Inova 600 NMR spectrometer. A ligand/protein ratio of 5 was obtained by diluting 6 mM BMOV and Na_3VO_4 stock in 50 mM sodium acetate (pH 5.0) containing 10% D_2O. 2D-^{15}N/^{1}H HSQC was recorded on the protein in the absence and presence of ligand. Significant chemical shift changes in the ^{15}N^{1}H-HSQC spectra of the protein on addition of the ligand indicated the binding of the ligands to the protein. The sequential resonance assignments in HCPTPA in the presence of phosphate were achieved by making use of a series of double and triple resonance NMR experiments [46].

2.7. X-ray crystallographic studies

Crystals of PTP1B C215S trap mutant (protein provided by Dr. Zhong-Yin Zhang Albert Einstein College of Medicine) were grown in 18–20% PEG 8000, Tris (pH 8.0), 1% BME at 4 °C using hanging drop vapor diffusion. Crystals appeared in ~1–2 weeks and were then used for soaking experiments. For soaking, BMOV was dissolved in water to a stock concentration of ~100 mM and added directly to the crystal drop to a final concentration of ~1 mM. Crystals were soaked at room temperature in room air for 2 h prior to data collection. Data were collected at beamline 17-ID (or 17-BM) in the facilities of the Industrial Macromolecular Crystallography Association Collaborative Access Team (IMCA-CAT) at the Advanced Photon Source. These facilities are supported by the companies of the Industrial Macromolecular Crystallography Association through a contract with Illinois Institute of Technology (IIT), executed through IIT's Center for Synchrotron Radiation Research and Instrumentation. Crystals were placed in 20% glycerol plus well solution and immediately frozen at 100 K. The structure was solved using Molrep and refined using Refmac, from the CCP4 programs, to 2.2 Å resolution [47].

3. Results

3.1. BMOV is a competitive, reversible PTP inhibitor

Enzyme/substrate competition assays demonstrated that

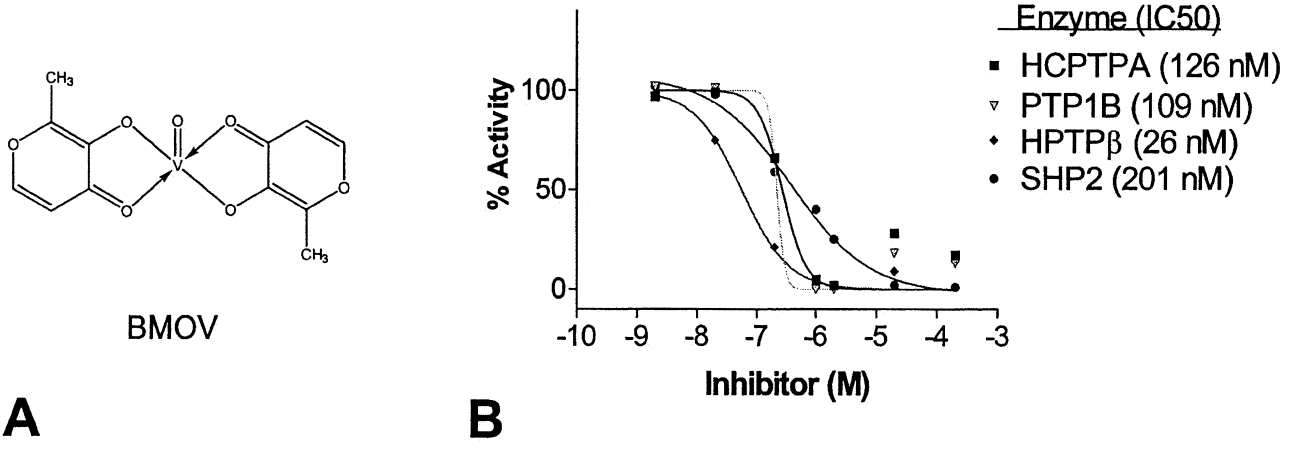

Fig. 1. BMOV is a nonselective protein tyrosine phosphatase inhibitor. (A) Molecular structure of BMOV (bismaltolatol oxovanadium). (B) Activity of BMOV at four different structurally diverse recombinant tyrosine phosphatases. Inset shows IC50 values.

BMOV, like other organovanadium compounds, was a potent, nonselective PTP inhibitor (Fig. 1). To gain further insight into the mechanism of action of BMOV, enzyme kinetic analysis was done against two structurally diverse PTPs, HCPTPA and PTP1B (Fig. 2). In these studies, BMOV demonstrated classical competitive inhibition against the fluorogenic substrate DiFMUP (6,8-difluoro-4-methylumbelliferyl phosphate) for both HCPTPA and PTP1B (KI = 0.79 μM and 0.90 μM, respectively). Thus, like sodium orthovanadate and other organovanadium compounds, BMOV is a nonselective, competitive PTP inhibitor.

Other organovanadium compounds such as bpV-phen (bis peroxo vanadium phenanthroline) oxidize the active site cysteine of PTP 'P-loop' and can function as irreversible PTP inhibitors [48]. To determine the propensity of BMOV to oxidize the active site cysteine, HCPTPA was incubated with either BMOV or bpV-phen and mass spectrometric analysis was done to determine alterations at the enzyme active site (Fig. 3). As anticipated, incubation of HCPTPA with bpV-phen at a 1:10 molar ratio caused a mass shift of 48 Daltons consistent with the oxidation of the P-loop cysteine to cysteic acid (SO_3) and this modification was confirmed by LC-ES-MS–MS (data not shown). At a 1:1000 molar ratio, incubation with bpV-phen resulted in generation of multiple higher molecular weight species suggesting the nonselective oxidation of multiple residues in addition to the P-loop cysteine. Conversely, incubation of HCPTPA with BMOV even at a molar ratio of 1:1000 failed to result in a mass shift, suggesting that BMOV, unlike bpV-phen does not irreversibly modify the enzyme.

3.2. BMOV inhibits intracellular phosphatase activity and enhances insulin receptor activation in vivo

Although organovanadium compounds inhibit isolated, recombinant PTPs, whether or not they inhibit intracellular phosphatase activity has been difficult to determine. In an attempt to measure inhibition of intracellular phosphatase activity, HEK293 cells were transfected with a vector directing the overexpression of PTP1B. The transfected cells overexpressed PTP1B as shown by western blot and by increased phosphatase activity as measured by the fluorescence of the cell permeable fluorogenic substrate DiFMUP (Fig. 4). Despite overexpression of PTP1B, >50% of the total cellular PTP activity was inhibited by 10 μm BMOV, consistent with its ability to readily cross the cell membrane and its activity against the isolated, recombinant enzyme.

Having shown that BMOV could inhibit intracellular phosphatase activity, its ability to enhance insulin receptor activation in vivo was tested. Briefly, insulin was administered to fasted rats with or without BMOV pretreatment. Insulin receptors were then isolated from heart tissue by immunoprecipitation and assayed for activation by antiphosphotyrosine immunoblot. In the absence of exogenous insulin, little if any increase in insulin receptor activation could be detected following BMOV treatment (Fig. 5). However, in the presence of insulin, receptor activation was enhanced after pretreatment with BMOV compared to animals treated with insulin only.

3.3. Uncomplexed vanadium is the active component of BMOV

In order to understand the mechanism of BMOV action at the molecular level, NMR studies were done with ^{15}N-labeled HCPTPA. Analysis of the chemical shift changes in the NMR spectrum of HCPTPA with either BMOV or Na_3VO_4 revealed that the changes corresponded to the residues forming the active site region of the protein, especially the consensus P-loop sequence (–^{12}CLGNICRS–). Surprisingly, BMOV and Na_3VO_4 caused essentially identical chemical shift changes of amide resonances in HCPTPA (Fig. 6). This suggests that the

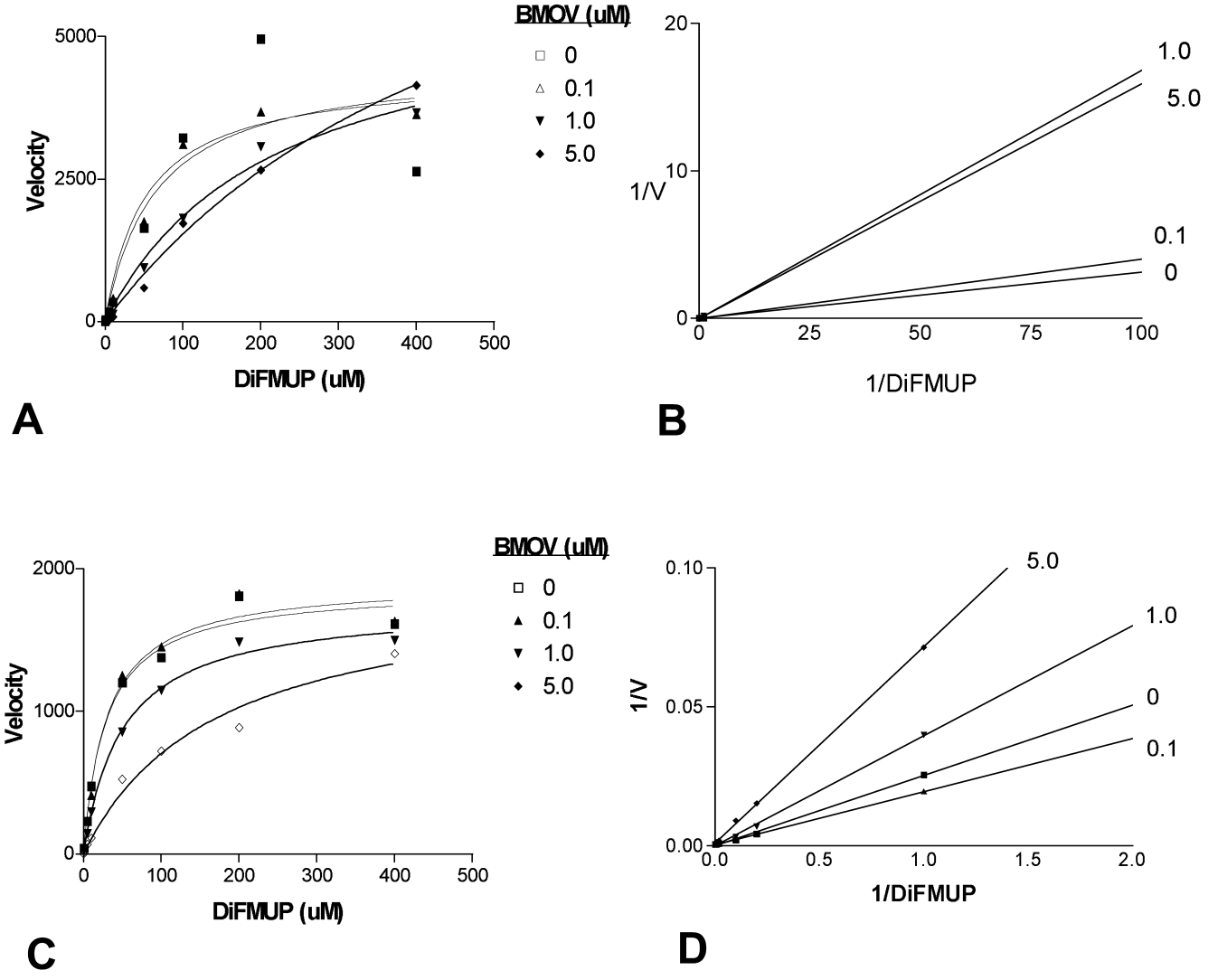

Fig. 2. BMOV is a competitive inhibitor of HCPTPA and PTP1B. Michaelis–Menten curves for HCPTPA (A) and PTP1B (C) in the presence of increasing concentrations of BMOV (see inset). Lineweaver–Burke analysis of data in panels A and C showing plots consistent with competitive inhibition of HCPTPA (B) and PTP1B (D).

protein experiences a similar chemical environment in the presence of the bound ligands and that uncomplexed vanadium (VO_4) from BMOV must be the binding moiety. Confirming this result, when BMOV was soaked into PTP1B crystals, only VO_4 could be fitted into the difference electron density and no other difference electron density was seen near the active site to indicate the intact BMOV molecule (Fig. 7A). The difference electron density unambiguously indicates that the geometry of VO_4 in the active site was that of a trigonal bipyramid with the base formed by three oxygen atoms and the apices formed by an oxygen and the hydroxyl group (Oγ) of serine 215. Interatomic distances between the vanadium atom and the oxygens appear to be unequal—the two axial distances are longer than the three equatorial ones. The vanadate ion was stabilized in the active site by a complex network of hydrogen bonds (Fig. 7B). The geometry and hydrogen binding network of the vanadate ion in the active site are consistent with previously published structures of vanadate with wild type PTP1b, *Yersinia* PTP and chloroperoxidase [49–51]. Resolution of the structure did not warrant unrestrained refinement, therefore the distances and angles of the oxovanadate ion were restrained to the values found in small molecules.

4. Discussion

In this report, we have explored the mechanism of phosphatase inhibition and insulin sensitization by BMOV, a unique organovanadium insulin mimetic. In previous studies, BMOV has been shown to be an effective antidiabetic agent in animal models of Type 2 diabetes, but little was known about its precise mechanism of action [33–

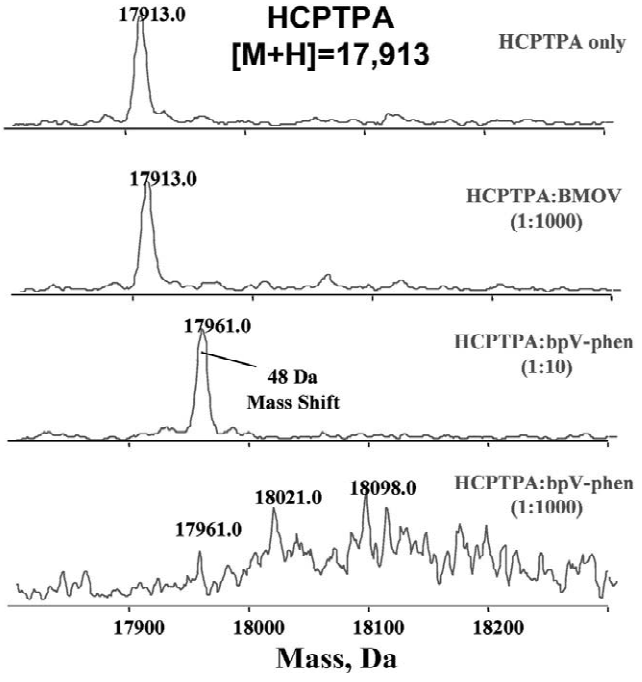

Fig. 3. BMOV does not irreversibly oxidize the active site of HCPTPA. HCPTPA samples were incubated with the indicated vanadium compounds and subjected to ESI-MS analysis to determine changes in the intact mass of the protein.

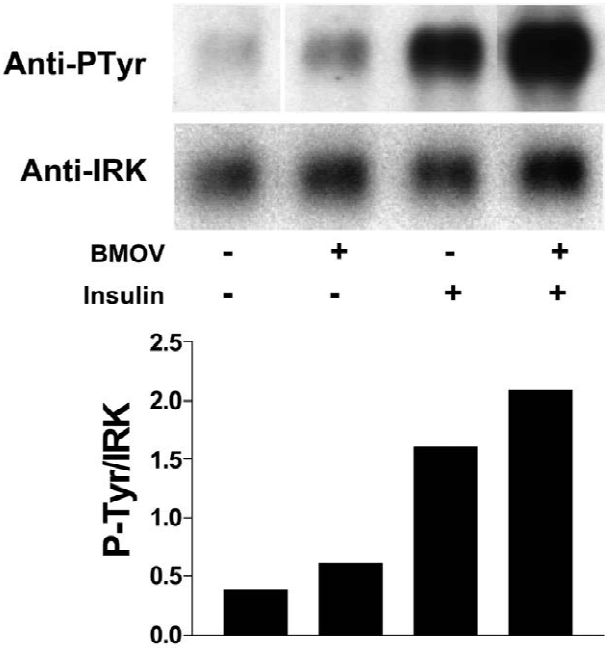

Fig. 5. BMOV enhances insulin receptor activation in vivo. Insulin receptors were isolated from heart tissue of animals treated acutely with insulin and/or BMOV and probed serially by western blot with anti-phosphotyrosine antibody (Anti-Ptyr) followed by an anti-insulin receptor β subunit antibody (Anti-IRK).

35,52,37]. Here we have demonstrated that, like other vanadium compounds, BMOV is a potent, competitive PTP inhibitor. Unlike some vanadium compounds, however, BMOV did not irreversibly oxidize the PTP active site suggesting it acts as a reversible inhibitor. A recent report demonstrated that BMOV treatment decreased PTP1B activity in skeletal muscle of diabetic rats supporting PTP inhibition as the mechanism of insulin sensitization [53]. Our studies showed that BMOV inhibited intracellular PTP1B activity and enhanced the autophosphorylation of the insulin receptor in vivo further supporting PTP inhibition as the mechanism of insulin sensitization.

In spite of enhanced insulin receptor activation by BMOV, previous studies have failed to identify the responsible downstream signaling pathways. For example, in a recent series of studies, the effects of vanadium compounds, including BMOV, were independent of the activation of PKC, PI3 kinase, PKB-α or glycogen synthase [54–56]. These results suggest either that other pathways downstream of the insulin receptor may be preferentially enhanced, i.e. the MAP kinase or cbl/CAP pathways, or

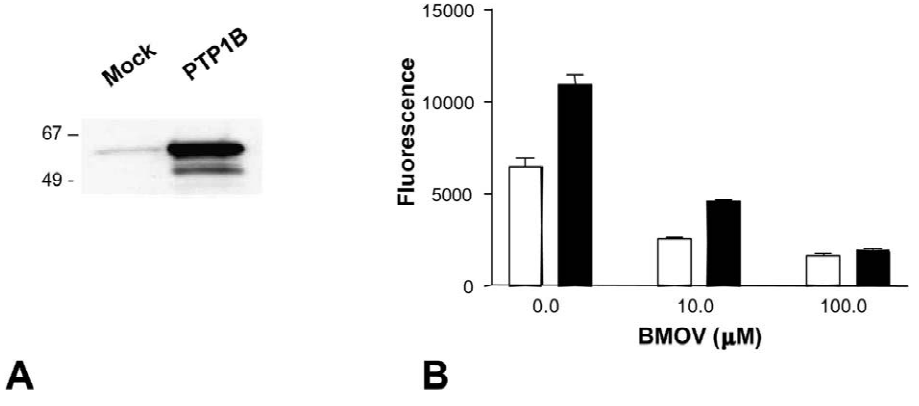

Fig. 4. BMOV inhibits PTP1B activity in cultured cells. A) Western blot showing overexpression of PTP1B in HEK 293 cells transiently transfected with a PTP1B plasmid vector. B) BMOV inhibits overexpressed PTP1B (black bars) and endogenous phosphatase activity (white bars) in HEK 293 cells.

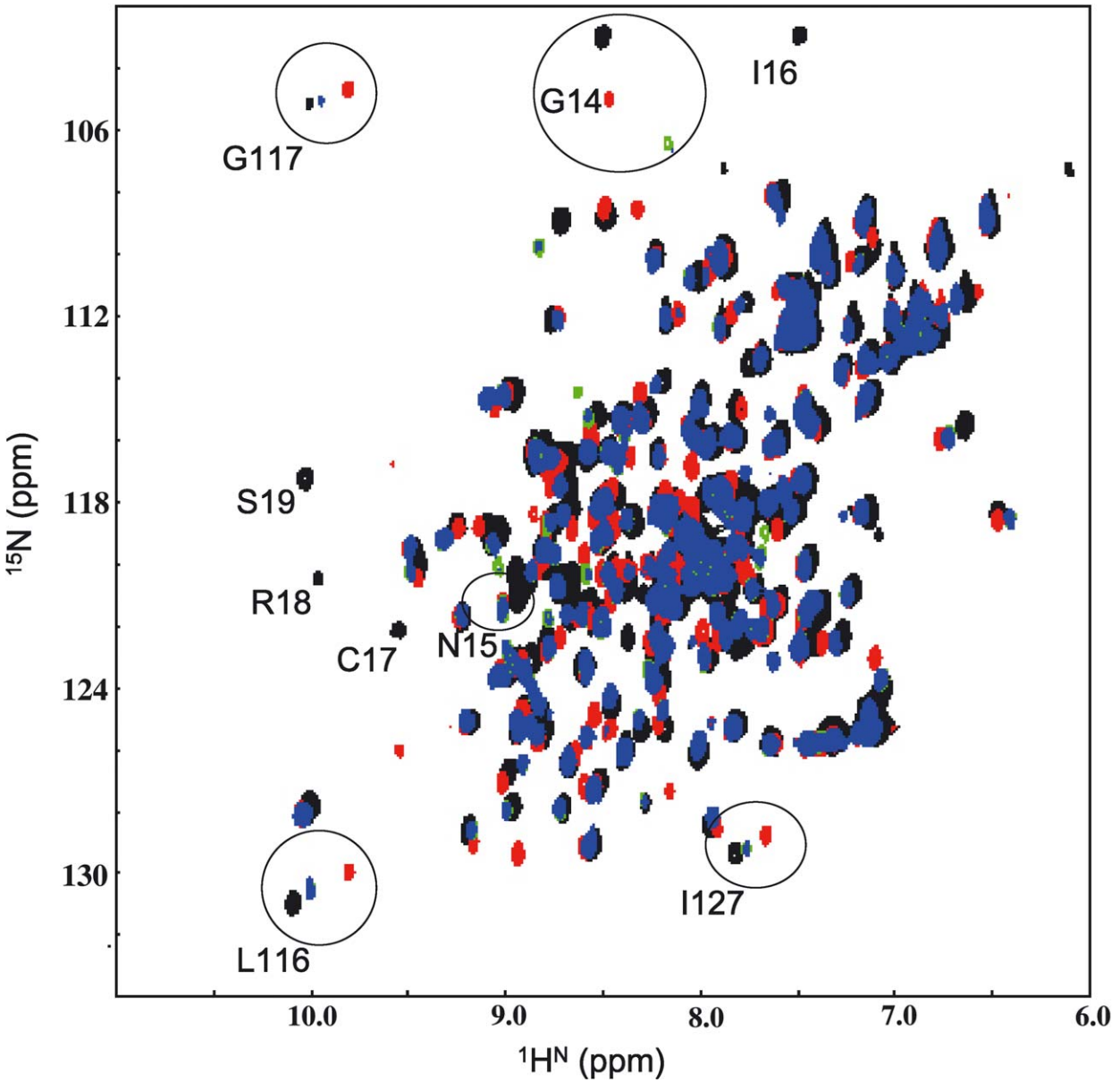

Fig. 6. NMR evidence for uncomplexed vanadate as the active component of BMOV. 2D-$^{15}N^{1}H$-HSQC spectra acquired on a ^{15}N-labeled sample of HCPTPA in the absence (red contours) and presence of BMOV (blue contours), NaOV (green contours), and phosphate (black contours). Similar chemical shift changes for residues in and around the active site (as labeled) are observed with BMOV and Na_3VO_4.

that there may be other mechanisms besides enhanced activation of the insulin receptor involved in BMOV action. Whatever the answer, considering the potent insulin sensitizing effects of BMOV and other organovanadium compounds, continued effort to further elucidate their mechanism of action could lead to important new insights into the regulation of insulin signaling and glucose metabolism.

Recent evidence suggests that varying the organic ligand in complex with vanadium can influence its bioactivity. Whether or not varying the ligand affects potency at the phosphatase enzyme or bioavailability of the compound has not been completely resolved. Some early data supported the idea that the organic ligand has its primary influence on absorption, tissue uptake and tissue distribution [27,57]. More recent data suggest that there may be little difference in the action of organovanadium compounds regardless of oxidation state or complexing ligand [58,31,24,59]. Our NMR and crystallographic data showing only vanadate in the active site demonstrate that, at least for BMOV, the organic ligand appears to play no role at the enzyme except perhaps as a delivery vehicle for vanadium.

Interestingly, recent studies have demonstrated that

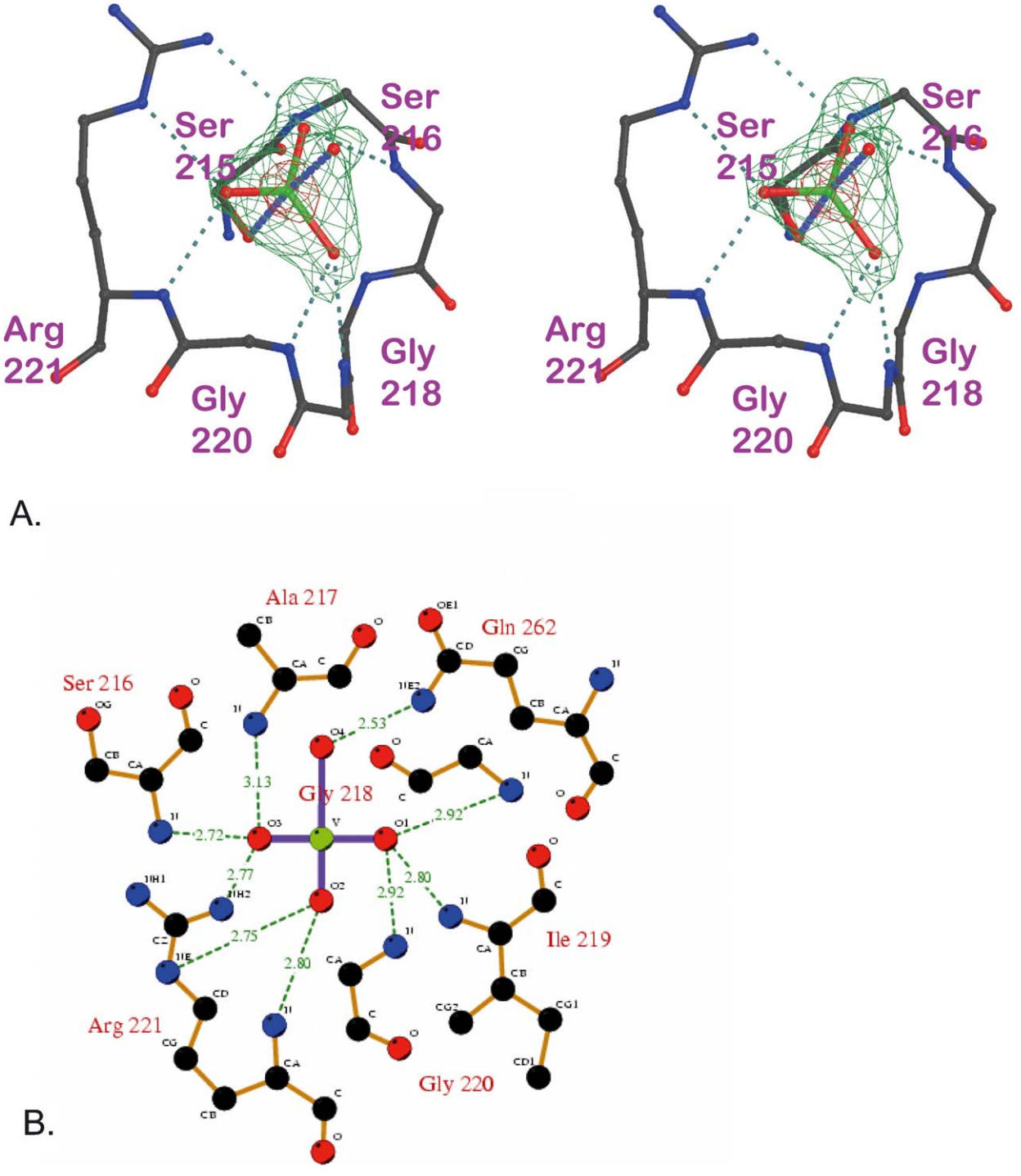

Fig. 7. Crystal structure of PTP1B (C215S mutant) soaked with BMOV reveals VO_4 coordinated to serine 215 in a trigonal bipyramidal geometry. (A) Stereo view of the difference electron density in the active site of PTP1B, shown together with the final model of the oxovanadate ligand. Most protein atoms are omitted for clarity, green electron density is contoured at 3.5 σ, red at 15.0 σ. Vanadium, oxygen, carbon, and nitrogen atoms are colored green, red, grey, and blue respectively. Axial vanadium–oxygen bonds are shown as thick broken blue lines, select hydrogen bonds between the ligand and the enzyme are shown as thin broken lines. (B) Detailed representation of the hydrogen bonding network of VO_4 with backbone atoms in the PTP1B (C215S mutant) active site. The interaction between VO_4 and the hydroxyl group of serine 215 has been omitted in order to clearly demonstrate the hydrogen bonding interactions. The plot panel B was generated using HBPLUSand LIGPLOT [69,70].

BMOV in aqueous solution is in equilibrium with free vanadium and maltol and that the proportion of uncomplexed vanadium increased with decreasing BMOV concentrations [60,61]. In addition, based on the kinetics of ligand substitution, it has been proposed that maltol would be readily replaced by stronger ligands in biological fluids

[62]. Moreover, in aqueous solution vanadium(IV) undergoes reversible oxidation to vanadium(V) [60,63]. Importantly, oxidation of BMOV would lead the formation of V(V) maltol complexes which may even more readily dissociate or undergo ligand replacement [63,62,60]. Whether or not the PTP active site might facilitate these events is a subject for future investigation.

Whatever the mechanism, our findings suggest that in 'physiologic' solutions, generation of VO_4 from BMOV is rapid enough to efficiently inhibit enzyme activity. Taken together, these data suggest that the most important effect of the organic ligands in organovanadium complexes may be on bioavailability and that ligand dissociation and oxidation to VO_4 may be required for efficient phosphatase inhibition. This is consistent with the fact that strong chelators such as EDTA inhibit the action of vanadium compounds and that there are still no structural studies documenting an organovanadium complex in a phosphatase active site [27].

Type 2 diabetes is an exploding worldwide epidemic. Although the pathophysiology of this disorder is complex, insulin resistance is an important component of the disease process. Thus, approaches to enhance insulin sensitization such as PPAR-γ agonism have gained much attention. More recently, PTP inhibition has emerged as another approach to enhance insulin sensitivity [64–68]. Vanadium compounds enhance insulin sensitivity and they are potent PTP inhibitors. Despite the ancillary role played by the organic ligand in the biological action of vanadium, thoughtful selection of the organic ligand could have important implications for the bioavailability of these compounds and for the clinical utility of vanadium for diabetes.

Acknowledgements

Use of the Advanced Photon Source was supported by the U. S. Department of Energy, Basic Energy Sciences, Office of Science, under Contract No. W-31-109-Eng-38.

References

[1] S.K. Hanks, A.M. Quinn, T. Hunter, Science 241 (1988) 42–52.
[2] J.E. Pessin, A.R. Saltiel, J. Clin. Invest 106 (2000) 165–169.
[3] A.R. Saltiel, Am. J. Physiol 270 (1996) E375–E385.
[4] A.R. Saltiel, J.E. Pessin, Trends Cell Biol. 12 (2002) 65–71.
[5] J. Schlessinger, Cell 103 (2000) 211–225.
[6] M.F. White, C.R. Kahn, J. Biol. Chem. 269 (1994) 1–4.
[7] F. Ahmad, R.V. Considine, B.J. Goldstein, J. Clin. Invest 95 (1995) 2806–2812.
[8] F. Ahmad, J.L. Azevedo, R. Cortright, G.L. Dohm, B.J. Goldstein, J. Clin. Invest 100 (1997) 449–458.
[9] D.T. Kulas, B.J. Goldstein, R.A. Mooney, J. Biol. Chem. 271 (1996) 748–754.
[10] P.M. Li, W.R. Zhang, B.J. Goldstein, Cell Signal. 8 (1996) 467–473.
[11] W.R. Zhang, P.M. Li, M.A. Oswald, B.J. Goldstein, Mol. Endocrinol. 10 (1996) 575–584.
[12] P. Chiarugi, P. Cirri, F. Marra, G. Raugei, G. Camici, G. Manao, G. Ramponi, Biochem. Biophys. Res. Commun. 238 (1997) 676–682.
[13] H. Chen, S.J. Wertheimer, C.H. Lin, S.L. Katz, K.E. Amrein, P. Burn, M.J. Quon, J. Biol. Chem. 272 (1997) 8026–8031.
[14] K.A. Kenner, E. Anyanwu, J.M. Olefsky, J. Kusari, J. Biol. Chem. 271 (1996) 19810–19816.
[15] M. Elchebly, P. Payette, E. Michaliszyn, W. Cromlish, S. Collins, A.L. Loy, D. Normandin, A. Cheng, H.J. Himms, C.C. Chan, C. Ramachandran, M.J. Gresser, M.L. Tremblay, B.P. Kennedy, Science 283 (1999) 1544–1548.
[16] L.D. Klaman, O. Boss, O.D. Peroni, J.K. Kim, J.L. Martino, J.M. Zabolotny, N. Moghal, M. Lubkin, Y.B. Kim, A.H. Sharpe, K.A. Stricker, G.I. Shulman, B.G. Neel, B.B. Kahn, Mol. Cell Biol. 20 (2000) 5479–5489.
[17] B.A. Zinker, C.M. Rondinone, J.M. Trevillyan, R.J. Gum, J.E. Clampit, J.F. Waring, N. Xie, D. Wilcox, P. Jacobson, L. Frost, P.E. Kroeger, R.M. Reilly, S. Koterski, T.J. Opgenorth, R.G. Ulrich, S. Crosby, M. Butler, S.F. Murray, R.A. McKay, S. Bhanot, B.P. Monia, M.R. Jirousek, Proc. Natl. Acad. Sci. USA 99 (2002) 11357–11362.
[18] D.C. Crans, M. Mahroof-Tahir, A.D. Keramidas, Mol. Cell Biochem. 153 (1995) 17–24.
[19] D.C. Crans, J. Inorg. Biochem. 80 (2000) 123–131.
[20] E. Tsiani, I.G. Fantus, Trends Endocrinol. Metab. 8 (1997) 51–58.
[21] S. Kadota, I.G. Fantus, G. Deragon, H.J. Guyda, B. Hersh, B.I. Posner, Biochem. Biophys. Res. Commun. 147 (1987) 259–266.
[22] S. Kadota, I.G. Fantus, G. Deragon, H.J. Guyda, B.I. Posner, J. Biol. Chem. 262 (1987) 8252–8256.
[23] B.I. Posner, R. Faure, J.W. Burgess, A.P. Bevan, D. Lachance, G. Zhang-Sun, I.G. Fantus, J.B. Ng, D.A. Hall, B.S. Lum, J. Biol. Chem. 269 (1994) 4596–4604.
[24] D. Rehder, P.J. Costa, C.F. Geraldes, M.M. Castro, T. Kabanos, T. Kiss, B. Meier, G. Micera, L. Pettersson, M. Rangel, A. Salifoglou, I. Turel, D. Wang, J. Biol. Inorg. Chem. 7 (2002) 675.
[25] Y. Shechter, S.J. Karlish, Nature 284 (1980) 556–558.
[26] E.L. Tolman, E. Barris, M. Burns, A. Pansini, R. Partridge, Life Sci. 25 (1979) 1159–1164.
[27] A.P. Bevan, J.W. Burgess, J.F. Yale, P.G. Drake, D. Lachance, G. Baquiran, A. Shaver, B.I. Posner, Am. J. Physiol 268 (1995) E60–E66.
[28] O. Blondel, D. Bailbe, B. Portha, Diabetologia 32 (1989) 185–190.
[29] R. Cordera, G. Andraghetti, R.A. DeFronzo, L. Rossetti, Endocrinology 126 (1990) 2177–2183.
[30] C.E. Heyliger, A.G. Tahiliani, J.H. McNeill, Science 227 (1985) 1474–1477.
[31] M. Melchior, S.J. Rettig, B.D. Liboiron, K.H. Thompson, V.G. Yuen, J.H. McNeill, C. Orvig, Inorg. Chem. 40 (2001) 4686–4690.
[32] J. Meyerovitch, Z. Farfel, J. Sack, Y. Shechter, J. Biol. Chem. 262 (1987) 6658–6662.
[33] U.A. Shinde, A.A. Mehta, R.K. Goyal, Indian J. Exp. Biol. 39 (2001) 864–870.
[34] J. Wang, V.G. Yuen, J.H. McNeill, Metabolism 50 (2001) 667–673.
[35] J. Yao, M.L. Battell, J.H. McNeill, Can. J. Physiol Pharmacol. 75 (1997) 83–90.
[36] V.G. Yuen, R.A. Pederson, S. Dai, C. Orvig, J.H. McNeill, Can. J. Physiol Pharmacol. 74 (1996) 1001–1009.
[37] V.G. Yuen, E. Vera, M.L. Battell, W.M. Li, J.H. McNeill, Diabetes Res. Clin. Pract. 43 (1999) 9–19.
[38] G. Swarup, S. Cohen, D.L. Garbers, Biochem. Biophys. Res. Commun. 107 (1982) 1104–1109.
[39] G. Huyer, S. Liu, J. Kelly, J. Moffat, P. Payette, B. Kennedy, G. Tsaprailis, M.J. Gresser, C. Ramachandran, J. Biol. Chem. 272 (1997) 843–851.
[40] X.Y. Wang, K. Bergdahl, A. Heijbel, C. Liljebris, J.E. Bleasdale, Mol. Cell Endocrinol. 173 (2001) 109–120.

[41] P.G. Drake, B.I. Posner, Mol. Cell Biochem. 182 (1998) 79–89.
[42] B.A. Reul, S.S. Amin, J.P. Buchet, L.N. Ongemba, D.C. Crans, S.M. Brichard, Br. J. Pharmacol. 126 (1999) 467–477.
[43] G.R. Willsky, A.B. Goldfine, P.J. Kostyniak, J.H. McNeill, L.Q. Yang, H.R. Khan, D.C. Crans, J. Inorg. Biochem. 85 (2001) 33–42.
[44] J.H. McNeill, V.G. Yuen, H.R. Hoveyda, C. Orvig, J. Med. Chem. 35 (1992) 1489–1491.
[45] Y.Y. Wo, M.M. Zhou, P. Stevis, J.P. Davis, Z.Y. Zhang, R.L. Van Etten, Biochemistry 31 (1992) 1712–1721.
[46] V.K. Rastogi, C.F. Diven, G.M. Seabrook, F.S. Genbauffe, R.T. Bechard, J.P. Fandl, K.G. Peters, J. Biomol. NMR 23 (2002) 251–252.
[47] Number 4 Collaborative Computational Project, Acta Cryst. D50 (1994) 760–763.
[48] C.J. Schofield, Z. Zhang, Curr. Opin Struct. Biol. 9 (1999) 722–731.
[49] J.M. Denu, D.L. Lohse, J. Vijayalakshmi, M.A. Saper, J.E. Dixon, Proc. Natl. Acad. Sci. USA 93 (1996) 2493–2498.
[50] A. Messerschmidt, R. Wever, Proc. Natl. Acad. Sci. USA 93 (1996) 392–396.
[51] A.D. Pannifer, A.J. Flint, N.K. Tonks, D. Barford, J. Biol. Chem. 273 (1998) 10454–10462.
[52] V.G. Yuen, R.A. Pederson, S. Dai, C. Orvig, J.H. McNeill, Can. J. Physiol. Pharmacol. 74 (1996) 1001–1009.
[53] A. Mohammad, J. Wang, J.H. McNeill, Mol. Cell Biochem. 229 (2002) 125–128.
[54] C.J. Band, B.I. Posner, J. Biol. Chem. 272 (1997) 138–145.
[55] L. Marzban, S. Bhanot, J.H. McNeill, Mol. Cell Biochem. 223 (2001) 147–157.
[56] E. Tsiani, E. Bogdanovic, A. Sorisky, L. Nagy, I.G. Fantus, Diabetes 47 (1998) 1676–1686.
[57] I.A. Setyawati, K.H. Thompson, V.G. Yuen, Y. Sun, M. Battell, D.M. Lyster, C. Vo, T.J. Ruth, S. Zeisler, J.H. McNeill, C. Orvig, J. Appl. Physiol. 84 (1998) 569–575.
[58] D.A. Barrio, M.D. Braziunas, S.B. Etcheverry, A.M. Cortizo, J. Trace Elem. Med. Biol. 11 (1997) 110–115.
[59] K.H. Thompson, Y. Tsukada, Z. Xu, M. Battell, J.H. McNeill, C. Orvig, Biol. Trace Elem. Res. 86 (2002) 31–44.
[60] Y. Sun, B.R. James, S.J. Rettig, C. Orvig, Inorg. Chem. 35 (1996) 1667–1673.
[61] G.R. Hanson, Y. Sun, C. Orvig, Inorg. Chem. 35 (1996) 6507–6512.
[62] E. Kiss, I. Fabian, T. Kiss, Inorg. Chim. Acta 340 (2002) 114–118.
[63] K. Elvingson, B.A. Gonzalez, L. Pettersson, Inorg. Chem. 35 (1996) 3388–3393.
[64] J. Burke-TR, Z.Y. Zhang, Biopolymers 47 (1998) 225–241.
[65] A. Cheng, N. Dube, F. Gu, M.L. Tremblay, Eur. J. Biochem. 269 (2002) 1050–1059.
[66] X. Espanel, S. Walchli, R.P. Gobert, M. El Alama, M.L. Curchod, N. Gullu-Isler, R.H. van Huijsduijnen, Endocrine 15 (2001) 19–28.
[67] A. Ostman, F.D. Bohmer, Trends Cell Biol. 11 (2001) 258–266.
[68] N.K. Tonks, B.G. Neel, Curr. Opin. Cell Biol. 13 (2001) 182–195.
[69] I.K. McDonald, J.M. Thornton, J. Mol. Biol. 238 (1994) 777–793.
[70] A.C. Wallace, R.A. Laskowski, J.M. Thornton, Protein Eng. 8 (1995) 127–134.